
Q2 USE CASE: VIBRATION ANALYSIS OF LARGE ROTATING MACHINERY

Óscar R. Enríquez, Gregory Prandaud, Eduardo Margallo

| Summary

In this use case, we show the capabilities of our Q2 system for vibration analysis of large rotating machinery. We scanned an electric generator operating in steady state at a nominal rotation rate of 3600 RPM, acquiring 101 scan frames with the 65 simultaneous laser channels of the Q2. Each frame contains 1 s of data sampled at 40 kHz, while the scan swept the azimuth angle from 0.0° to 46.0° in 0.46° steps. A shaft tachometer produced one pulse per revolution and fed Q2's analog input. We used that tach signal to estimate RPM per frame and to reference order phase consistently from frame to frame.

We report tach-derived speed, global amplitude spectral density, order amplitude and tach-referenced phase maps for orders 1–8, plus a diagnostic partition of band-limited vibration energy into order-synchronous versus residual (“asynchronous”) content.

| Introduction

Q2 is Ommatidia's multi-channel laser Doppler vibrometer (LDV) combined with a scanning metrology system. In vibrometry mode, each of the 65 beams measures line-of-sight (LOS) surface velocity at its measurement point. In metrology mode, Q2 measures distance and builds a 3D point cloud of the scene. By rotating the sensor head in azimuth, we sweep the 65-point vertical line across the field of view and build frame×channel maps that spatially resolve vibration response over the observed portion of the assembly.

Q2 operates in two main modes:

- **Vibrometry mode**, which measures surface velocity, and
- **Metrology mode**, which measures distance and builds a 3D point cloud of the scene.

The system uses multichannel coherent detection and a frequency-modulated continuous-wave (FMCW) laser source. This architecture supports measurement of vibration and distance at all 65 channels, enabling three-dimensional characterisation of dynamic behaviour. In addition, Q2

integrates Ommatidia's SpeckleGuard™ speckle-management algorithms, which stabilise LDV data on difficult, rough or low-reflectivity surfaces, and the DOLL™ digital optical locked loop, which extends the usable velocity range of the vibrometer by a 10x factor.

Key capabilities relevant for NVH investigations include:

- sampling up to 40 kHz across 65 parallel channels,
- a standard velocity range of ± 15.5 mm/s in LDV mode, expandable with DOLL™,
- fast scanning over large azimuthal angles to map the full field of view, and
- open HDF5 data format for integration into existing analysis workflows.

The instrument is controlled from Ommatidia Atelier™, which handles configuration, acquisition, and export. For data analysis we used a pre-release version of the vibration-processing pipeline developed in Python.

Measurement objectives

This project aimed to evaluate whether Q2 can support vibration analysis on large rotating machinery under realistic test conditions. We set out to:

Verify adequate optical return across the intended field of view before vibration acquisition.

Acquire spatially dense vibration data using Q2's 65 channels while scanning the generator.

Use a one-pulse-per-rev shaft tachometer (captured on Q2) to track speed per frame and define a phase reference.

Produce order response maps (amplitude and tach-referenced phase) for orders 1–8 and provide summary views that facilitate expert interpretation.

Provide an initial diagnostic estimate of residual, non-order vibration energy to guide discussion and validation.

Methods

DUT and sensor positioning

Q2 projected a vertical line of 65 infrared measurement points on the DUT. We then swept the azimuth angle to scan horizontally across the assembly and form two-dimensional maps (see figure 1). In all frame×channel maps, the horizontal axis corresponds to scan position (frame index), and the vertical axis corresponds to channel index (vertical position). The scan swept azimuth from 0.0° to 46.0° in 0.46° steps; therefore, frame index k corresponds approximately to azimuth angle $\varphi \approx (k-1) \cdot 0.46^\circ$ over the $0-46^\circ$ range. Q2 operated at an approximate standoff distance of 1.6 m from the front corner of the generator. The surface remained untreated since we verified that there was enough optical signal reflected from the DUT by performing a quick intensity scan (figure 2).

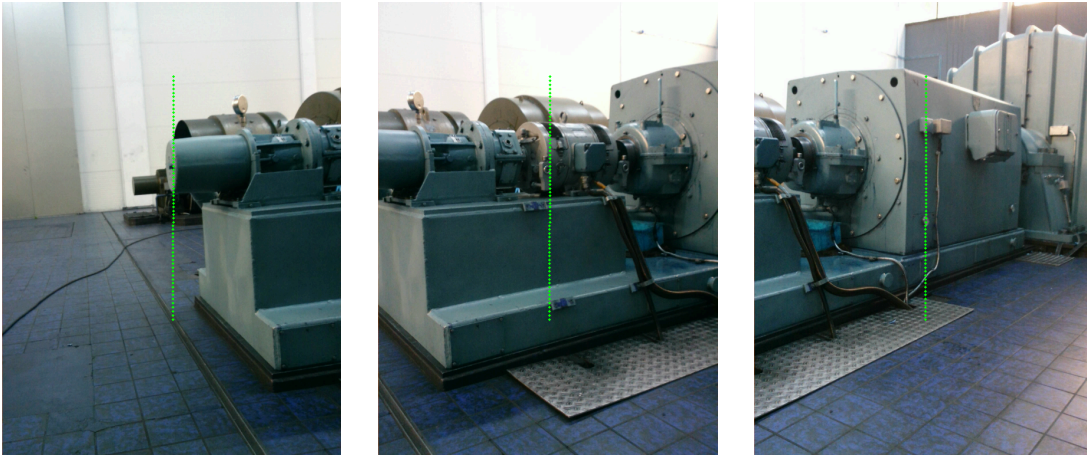


Figure 1. View from Q2's RGB camera at the start, middle and end of the scan. Green points represent the virtual positions of the 65 infrared laser channels.

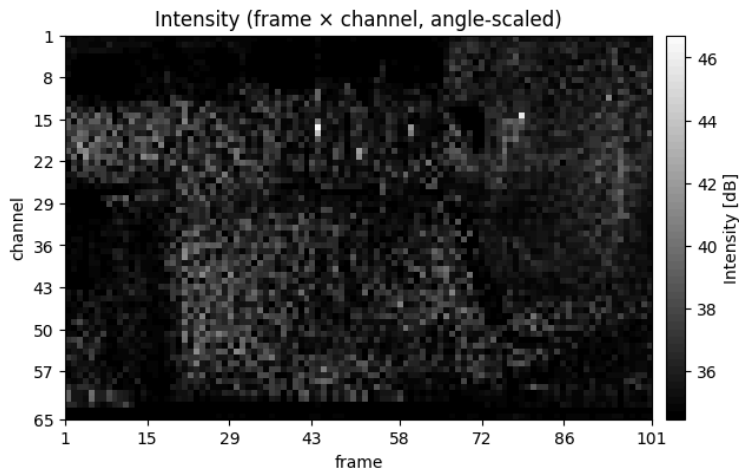


Figure 2. Optical return intensity recorded during a quick acquisition-quality sweep used to verify sufficient reflected signal across the scan. This figure does not represent vibration.

Operation conditions

The generator operated in steady state near a nominal 3600 RPM during the scan. Small frame-to-frame speed variation is visible in the tach-derived RPM estimate (fig. 4), and we use the per-frame tach-derived rotation rate for order analysis.

Data processing

We processed the Q2 data as follows:

1. **Load data and scan geometry.** We loaded multi-channel complex phasor frames from Q2 and used scan metadata to keep a consistent mapping between scan position (frame index) and

channel index (vertical position). Each frame contains **1 s** of data sampled at **40 kHz (101 frames total)**.

2. **Demodulate to velocity.** We demodulated each complex phasor trace to a velocity time series (mm/s) using a PLL-based phase-rate estimator. During development, we monitored a wrapped phase-error diagnostic as a lock/quality indicator; the report focuses on the vibration-analysis outputs.
3. **Compute a global ASD summary and detect peak candidates.** For each scan point (frame \times channel), we compute a one-sided velocity PSD from the 1 s record and express it as ASD = $\sqrt{\text{PSD}}$ in mm/s/ $\sqrt{\text{Hz}}$. We then aggregate ASD across all scan points at each frequency to obtain p50 and p95 curves. In addition, we compute a power-consistent global mean in ASD units as $\text{meanPow} = \sqrt{\text{mean PSD}}$ (i.e., PSDs are averaged first, then square-rooted). Peak candidates are detected on the p95 curve using a prominence criterion evaluated in dB, yielding the marker frequencies shown in Figure 5. Under steady operation near 3600 RPM, the first eight peak candidates lie near $n f_{\text{rot}}$ (for $n = 1, \dots, 8$), matching the order set analyzed later via tach-referenced order tracking.
4. **Extract tach and estimate speed.** For each frame, we detected tach rising edges and computed an RPM estimate from the pulse timing. We define the tach event as the **first detected rising-edge threshold crossing** within each 1 s record (sub-sample interpolated), and we use its time t_0 as the per-frame phase reference.
5. **Estimate selected order coefficients via synchronous detection.** Instead of angle-resampling, we estimated orders by projecting each 1 s velocity record onto complex exponentials at integer multiples of the tach-derived rotation frequency f_{rot} . This yields complex coefficients for the specified discrete orders (here: **1–8**), rather than a full order spectrum. Because this approach does not resample to constant angle, it assumes speed is approximately constant within each 1 s record; strong intra-record speed modulation would motivate angle-domain resampling or a more advanced order-tracking method. We reference phase by rotating each coefficient so that phase zero aligns with the first detected tach rising edge within that frame.
6. **Build order amplitude and phase maps with amplitude-based masking.** We computed amplitude maps as $|C|$, the estimated peak velocity amplitude of the order component (mm/s). Phase maps correspond to $\angle C$, where we masked phase where low amplitude makes phase noise-dominated. We set a per-channel amplitude threshold at 8% of $|C|$ over tach-valid frames, enforced an absolute minimum floor of **0.009 mm/s**, and applied Gaussian smoothing ($\sigma = 0.6$) to the amplitude field used for the mask decision to reduce speckle. Masked pixels appear white.
7. **Compute residual (“asynchronous”) fraction as an energy-partition diagnostic.** We compute total vibration energy as band-limited RMS velocity over **0–3000 Hz** from PSD-consistent integration of the velocity spectrum, and we express it as power $P_{\text{total}} = v_{\text{rms}}^2$. We estimate order-synchronous energy from the complex order coefficients for orders **1x–8x** using the proxy

$$P_{\text{orders}} = \sum_{n \in \{1..8\}} |C_n|^2.$$

Because P_{total} and P_{orders} do not share a guaranteed absolute scale (windowing and estimator differences), we apply a robust scalar alignment **per processing block** (we load the dataset piecewise), based on global medians over all frames and channels in that block:

$$\beta = \frac{\text{median}(P_{\text{total}})}{\text{median}(P_{\text{orders}})}, \quad P_{\text{orders,scaled}} = \beta P_{\text{orders}}.$$

We then compute the residual (“asynchronous”) energy as

$$P_{\text{async}} = \max(P_{\text{total}} - P_{\text{orders,scaled}}, 0),$$

and we report it as RMS velocity via $\text{order_rms} = \sqrt{P_{\text{orders,scaled}}}$ and $\text{async_rms} = \sqrt{P_{\text{async}}}$. In Figure 8 we plot the RMS ratio $\text{async_rms} / v_{\text{rms}}$ (a bounded [0,1] quantity). Note that this residual is defined as non-(1×–8×) content in the 0–3000 Hz band and can include higher integer orders (>8×) as well as broadband/non-synchronous vibration; it is not a pure “asynchronous only” estimator.

Conventions used in this report

- **Velocity** is **line-of-sight (LOS)** surface velocity reported in **mm/s**.
- For order n , the complex coefficient C_n is estimated by synchronous detection at $n \cdot f_{\text{rot}}$ (per frame). **Amplitude maps show** $|C_n|$ and **phase maps show** $\arg(C_n)$ after tach referencing.
- **Amplitude convention:** the synchronous-detection scaling yields an estimate of the **peak sinusoidal amplitude** at that order. (For a pure sinusoid, RMS would be $|C_n|/\sqrt{2}$.)
- **Phase reference:** per frame, phase zero is aligned to the **first detected tach rising edge** within that 1 s record.
- **Residual (“async”) metric:** computed in the **0–3000 Hz** band as a bookkeeping residual relative to orders **1×–8×**; it can include **higher orders (>8×)** and other non-(1×–8×) content. It is therefore not a pure “asynchronous-only” estimator.

Results and interpretation

Figure 1 shows Q2 camera views at the start, middle, and end of the scan and illustrates the scanned field of view and the 65-channel line on the DUT.

Figure 2 shows the optical return intensity during the initial acquisition-quality sweep. We include it only to document adequate reflected signal across the scan; it does not represent vibration amplitude.

Figures 3 and 4 summarize the tach reference. Figure 3 shows a representative tach waveform captured by Q2 (one pulse per revolution). Figure 4 shows the RPM estimate per frame derived from tach timing; we use it as f_{rot} for the order analysis.

Figure 5 provides a compact frequency-domain overview of the vibration response during steady operation near 3600 RPM (shaft frequency $f_{\text{rot}} \approx 60$ Hz). The separation between the p50 and p95

curves indicates pronounced spatial non-uniformity: most scan points exhibit comparatively moderate broadband levels, while a subset of locations shows substantially higher response at discrete frequencies.

Importantly, the lowest-frequency peak candidates (blue markers) align with the order-tracking analysis used later in this report: the first eight peaks occur near $n f_{\text{rot}}$ for $n = 1, \dots, 8$ and therefore correspond to orders $1\times\text{--}8\times$ mapped in Figures 6 and 7. In this sense, the global ASD peak-picking acts as a consistency check and a prioritization step: it highlights the dominant tonal components present in the upper tail of the spatial distribution and motivates the subsequent tach-referenced estimation of complex order coefficients C_n (amplitude $|C_n|$ and phase $\arg(C_n)$).

Figures 6 and 7 show order-response maps for orders 1–8. The amplitude maps highlight spatial variation of order-synchronous vibration content across scan position and channel. The phase maps show tach-referenced phase relative to the first tach rising edge in each frame; we mask low-amplitude regions to avoid displaying phase of noise.

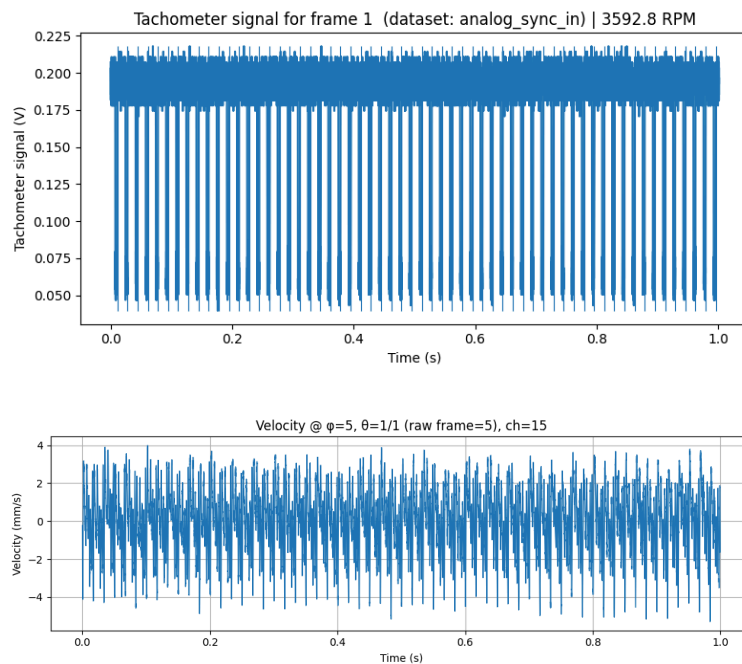


Figure 3. Representative time-domain signals for one scan frame. (top) Shaft tachometer waveform captured on the Q2 analog input (one pulse per revolution). (bottom) Demodulated line-of-sight velocity time trace (mm/s) for a representative channel in the same frame (1 s record at 40 kHz).

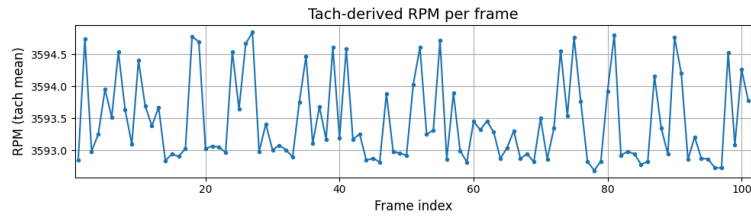


Figure 4. Tach-derived rotation rate estimate (RPM) per scan frame, computed from tach pulse timing.

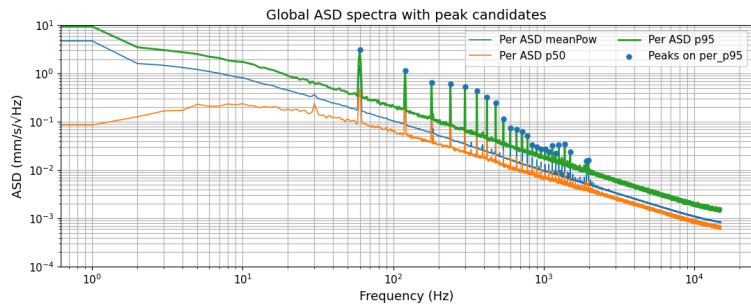


Figure 5. Global velocity ASD with peak candidates (nominal ~ 3600 RPM). Global amplitude spectral density (ASD) of line-of-sight (LOS) surface velocity, aggregated across all scan points (101 frames \times 65 channels). The median (p50) curve represents the typical response across the scanned field of view, meanPow ($\sqrt{\text{mean PSD}}$) represents a power-consistent global average expressed in ASD units, and p95 captures the upper-end response associated with spatial hotspots / strongly excited regions. Blue markers indicate peak candidates detected on the p95 curve (prominence evaluated in dB). The first eight peak candidates fall near integer multiples of the tach-derived rotation frequency f_{rot} and correspond to orders $1\times$ – $8\times$ analyzed in the tach-referenced order maps shown later.

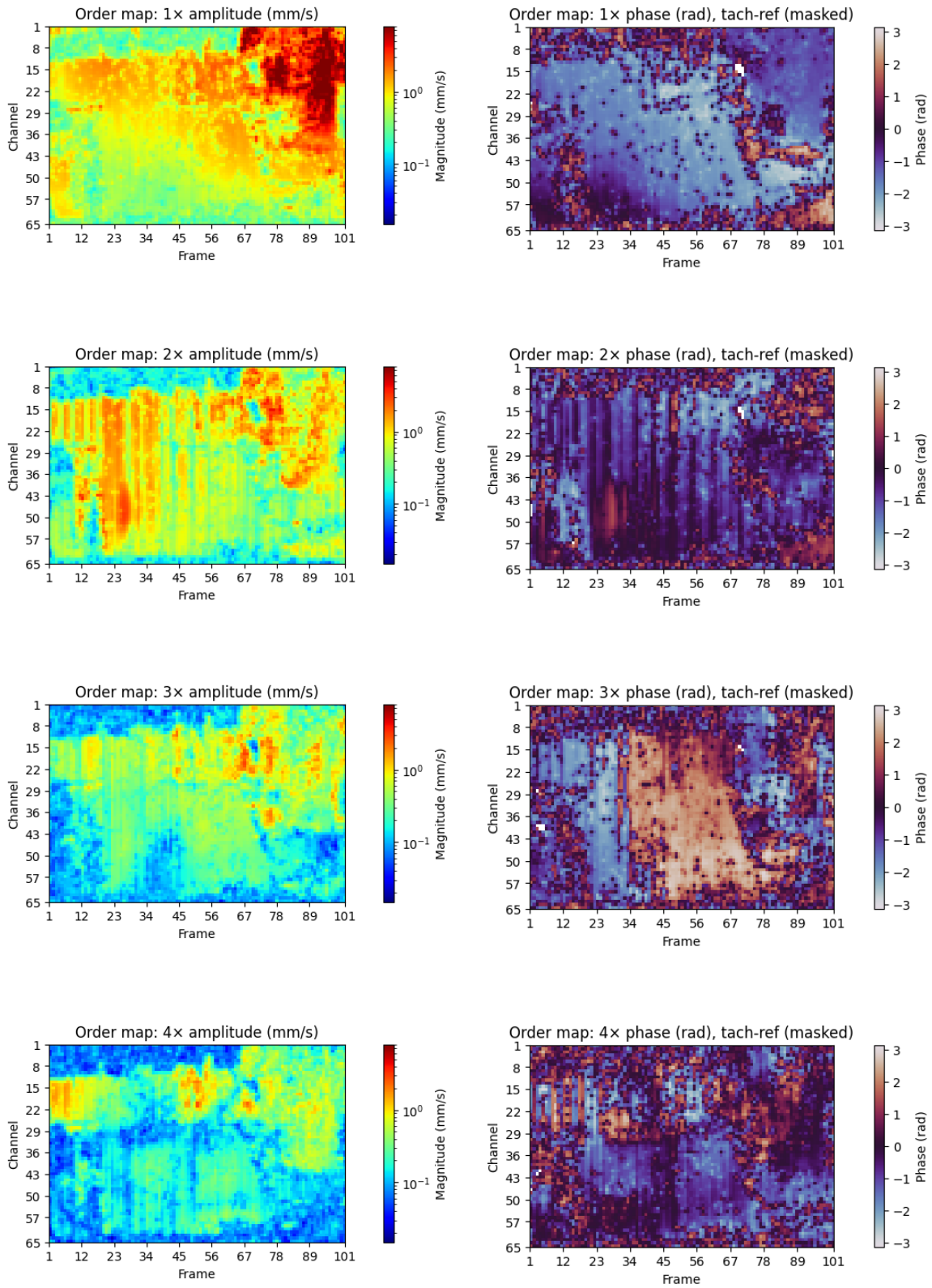


Figure 6. Tach-referenced order-response maps for orders 1–4. Amplitude shows $|C|$; phase shows $\arg(C)$ referenced to the first tach rising edge within each frame. Phase is masked where amplitude is below the per-channel threshold (masked pixels in white).

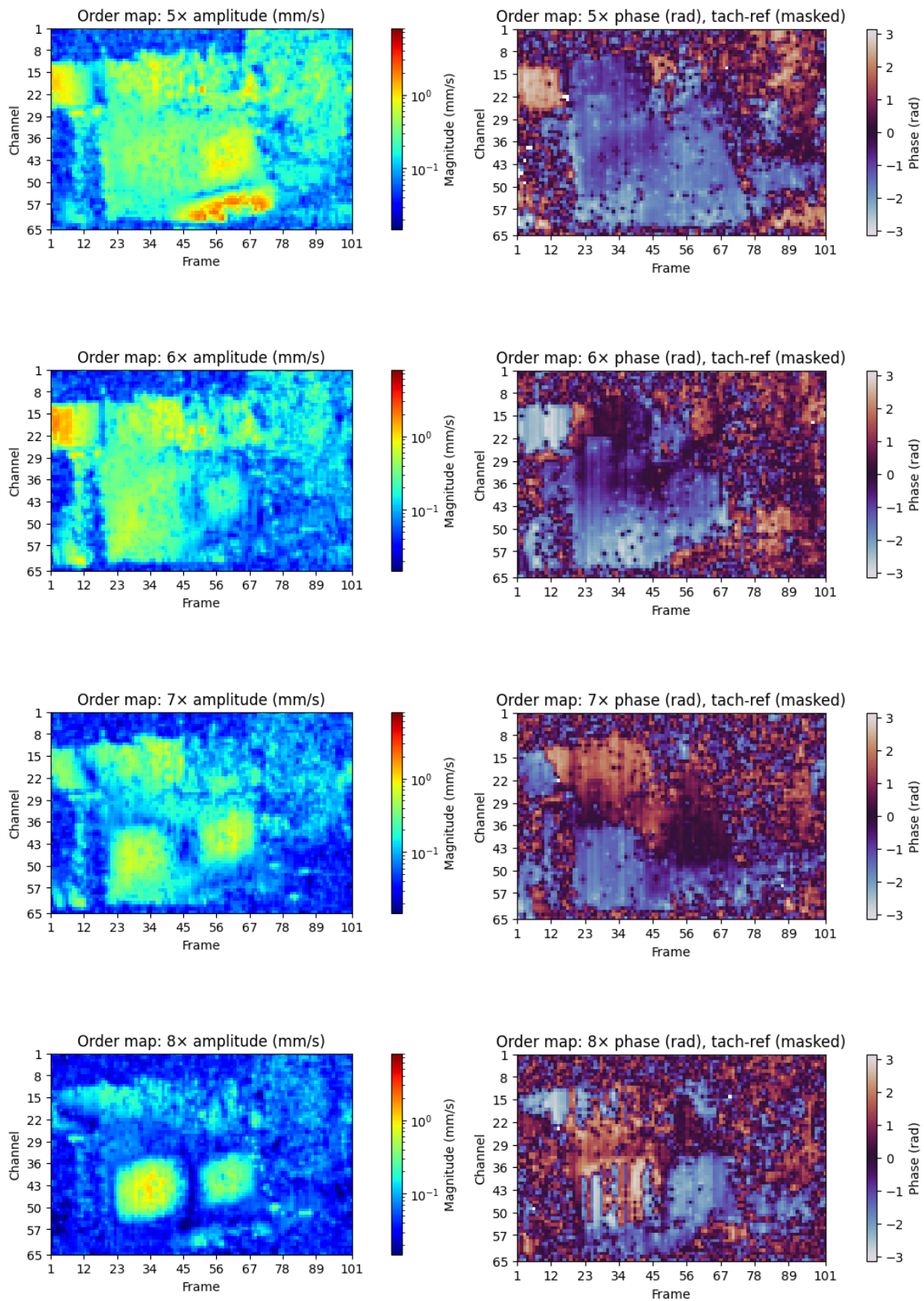


Figure 7. Tach-referenced order-response maps for orders 5–8 (same conventions as Figure 6).

Figure 7 provides a global summary of order content using a robust aggregation over frames and channels.

Figure 8 shows the residual (“asynchronous”) fraction map, which estimates the **0–3000 Hz** band-limited energy not explained by orders **1–8** after **processing-block** median-based scalar alignment between PSD-derived energy and the coefficient-based energy proxy. Note that large regions of high residual fraction occur at scan locations that fall outside the generator body when compared against the camera views and beam placement in Figure 1. In particular, bottom channels during approximately frames 1–20 and top channels up to approximately frame 60 correspond to background / fixture / off-DUT points.

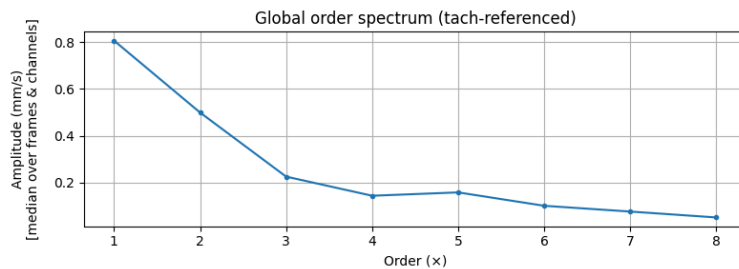


Figure 8. Global order summary derived from robust aggregation of order coefficients over frames and channels.

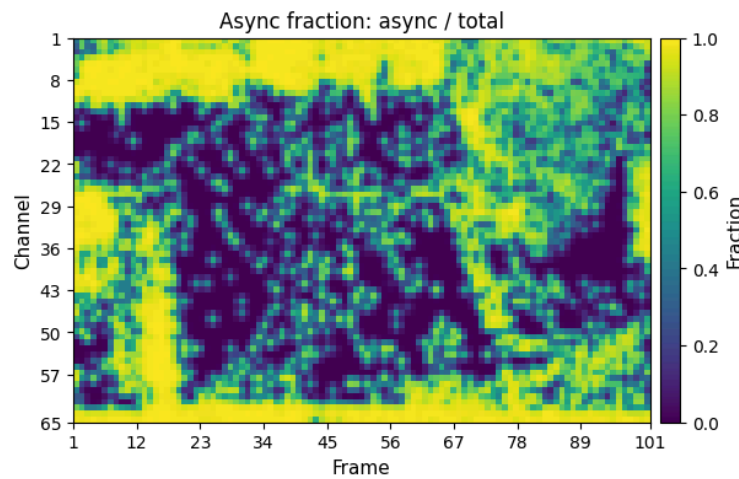


Figure 9. Residual (“asynchronous”) fraction map: diagnostic estimate of **0–3000 Hz** band-limited vibration energy not explained by orders **1–8**. We align the PSD-based and coefficient-based energy scales using a robust scalar: $\beta = \text{median}(P_{total}) / \text{median}(P_{orders})$ with: $P_{total} = v_{rms}^2$ (computed from the PSD-integrated 0–3000 Hz band) $P_{orders} = \sum_{n=1}^8 |C_n|^2$

Conclusions

Q2 acquired spatially dense vibrometry data on a large generator operating in steady state at nominal 3600 RPM. The measurement used 101 scan frames (1 s per frame at 40 kHz) and a 0–46° azimuth sweep in 0.46° steps at an approximate 1.6 m standoff distance. A shaft tachometer (one pulse per revolution), captured on Q2's analog input, provided the reference needed to estimate RPM per frame and to compute tach-referenced order maps.

The presented maps and summary metrics provide an initial view of order-synchronous vibration patterns for orders 1–8, together with a diagnostic estimate of residual (non-order) vibration energy in the 0–3000 Hz band. The analysis estimates selected orders via synchronous detection in the time domain and uses explicit masking rules to display phase only where amplitude supports meaningful phase interpretation. The residual metric applies a robust scalar alignment per processing block before computing an energy-difference residual; it supports energy bookkeeping in-band and does not reconstruct a time-domain residual signal.